

# Quantum confinement effects in hydrogen-intercalated $\text{Ga}_{1-x}\text{As}_x\text{N}_x\text{-GaAs}_{1-x}\text{N}_x\text{:H}$ planar heterostructures investigated by photoluminescence spectroscopy

R. Trotta,<sup>1</sup> L. Cavigli,<sup>2</sup> L. Felisari,<sup>3</sup> A. Polimeni,<sup>1,\*</sup> A. Vinattieri,<sup>2</sup> M. Gurioli,<sup>2</sup> M. Capizzi,<sup>1</sup> F. Martelli,<sup>3,4</sup> S. Rubini,<sup>3</sup> L. Mariucci,<sup>4,5</sup> M. Francardi,<sup>5</sup> and A. Gerardino<sup>5</sup>

<sup>1</sup>CNISM, Dipartimento di Fisica, Sapienza Università di Roma, P.le A. Moro 2, 00185 Roma, Italy

<sup>2</sup>CNISM, Unità di Ricerca di Firenze and Department of Physics, Via Sansone 1, 50019 Sesto Fiorentino, Italy

<sup>3</sup>TASC-INFN-CNR, Area Science Park, S.S. 14, Km. 163.5, 34012 Trieste, Italy

<sup>4</sup>IMM-CNR, via del Fosso del Cavaliere 100, 00133 Roma, Italy

<sup>5</sup>IFN-CNR, via Cineto Romano 42, 00156 Roma, Italy

(Received 28 May 2010; published 29 June 2010)

Carrier quantum confinement has been achieved in dilute nitrides by controlling the peculiar kinetics of hydrogen in those materials.  $\text{GaAs}_{1-x}\text{N}_x/\text{GaAs}_{1-x}\text{N}_x\text{:H}$  planar heterostructures have been fabricated by deposition of submicrometer titanium wires (width  $w=485$ ,  $175$ , and  $80$  nm) on  $\text{GaAs}_{1-x}\text{N}_x$  and subsequent H irradiation. Continuous-wave photoluminescence, PL, in ensembles of  $\text{GaAs}_{1-x}\text{N}_x/\text{GaAs}_{1-x}\text{N}_x\text{:H}$  heterostructures shows a blueshift of the PL peak energy and a marked increase in the PL radiative efficiency with decreasing one of the wire dimensions down to the nanometer-scale length. Concomitantly, time-resolved microphotoluminescence in single structures exhibits a pronounced slow down of carrier relaxation toward the ground state. All these results, supported by numerical calculations of H diffusion profiles, indicate that carrier quantum confinement can be achieved by H engineering of dilute nitrides.

DOI: [10.1103/PhysRevB.81.235327](https://doi.org/10.1103/PhysRevB.81.235327)

PACS number(s): 78.66.Fd, 71.55.Eq, 78.47.-p, 78.55.Cr

## I. INTRODUCTION

The synthesis of nanostructured semiconductors is incessantly boosting the number of opportunities in the field of electronics and photonics. The control and modification of the physical properties of semiconductor heterostructures at nanometer scale lengths can be obtained by several approaches<sup>1</sup> comprising self-assembly,<sup>2</sup> site-controlled growth,<sup>3</sup> vapor-liquid-solid growth,<sup>4</sup> etc. These approaches are particularly effective when combined with materials, whose physical properties can be tailored on purpose. An example is provided by dilute nitride semiconductors, such as  $\text{GaAs}_{1-x}\text{N}_x$  and  $\text{GaP}_{1-x}\text{N}_x$ ,<sup>5</sup> whose electronic (e.g., band gap energy, electron mass and  $g$  factor)<sup>6–10</sup> and structural (e.g., lattice constant)<sup>11–13</sup> characteristics are strongly modified by postgrowth hydrogen incorporation. Indeed, the formation of specific nitrogen-hydrogen complexes<sup>13</sup> removes in a fully controllable and reversible manner the strong effects produced by N-alloying of III-V compounds and alloys. Furthermore, H incorporation can be spatially tailored via prior deposition of H-opaque Ti masks.<sup>14–16</sup> In this way, a modulation of the band gap energy in the crystal growth plane was achieved<sup>14</sup> and a polarization control of the emitted light was demonstrated in strain-engineered  $\text{GaAs}_{1-x}\text{N}_x/\text{GaAs}_{1-x}\text{N}_x\text{:H}$  heterostructures.<sup>17</sup> It would be even more attractive to pattern H-induced effects down to the nanometer scale in order to fabricate shape-, size-, and site-controlled nanostructures.

In this work, we report on continuous-wave and time-resolved photoluminescence, PL, measurements in single and ensembles of  $\text{GaAs}_{1-x}\text{N}_x/\text{GaAs}_{1-x}\text{N}_x\text{:H}$  heterostructures obtained by hydrogen diffusion into a  $\text{GaAs}_{1-x}\text{N}_x$  epilayer, covered with titanium wires having different width ( $w=485$ ,  $175$ , and  $80$  nm). In the narrowest wires, optical measurements show a blueshift of the ground state energy and an

increase in the PL radiative efficiency, together with band-filling effects and a slow down in the carrier relaxation toward the ground state. These results are the first reported signature of carrier quantum confinement in  $\text{GaAs}_{1-x}\text{N}_x/\text{GaAs}_{1-x}\text{N}_x\text{:H}$  planar heterostructures. Simulations of H diffusion confirm that the carrier confining profile progressively reduces in size along the growth axis and attains the carrier de Broglie wavelength in the case of the  $w=80$  nm wires.

## II. EXPERIMENT

We studied a 200 nm-thick  $\text{GaAs}_{1-x}\text{N}_x$  layer (nitrogen concentration equal to 0.9%) grown at 500 °C by molecular-beam epitaxy on top of a GaAs buffer deposited at 600 °C on a (001) GaAs substrate. A 50 nm-thick film of titanium was deposited on the sample surface and patterned by electron-beam lithography as to obtain  $800 \times 800 \mu\text{m}^2$  ensembles of Ti wires. These latter were 485, 175, and 80 nm wide, and 5  $\mu\text{m}$  far apart each other, as determined by a scanning electron microscope. The patterned sample was hydrogenated at 300 °C by a low-energy (100 eV) ion beam. Wires with different width are deposited on a same chip so that the same hydrogenation conditions are established for all wire ensembles. A comparison between atomic force microscopy measurements performed on as-deposited Ti wires and H-irradiated Ti wires (under the same conditions used for the other hydrogenated structures) have provided no evidence of Ti blistering produced by hydrogenation. Only a likely slight surface roughening in the H-irradiated structure has been observed that does not affect the results presented here.

Once removed the Ti mask, macro-PL was excited by a 532 nm laser, spectrally analyzed by a 0.75 m monochromator and detected by a charge-coupled device (CCD) detector. For time-resolved micro-PL ( $\mu\text{-PL}$ ) a dye laser ( $\lambda$

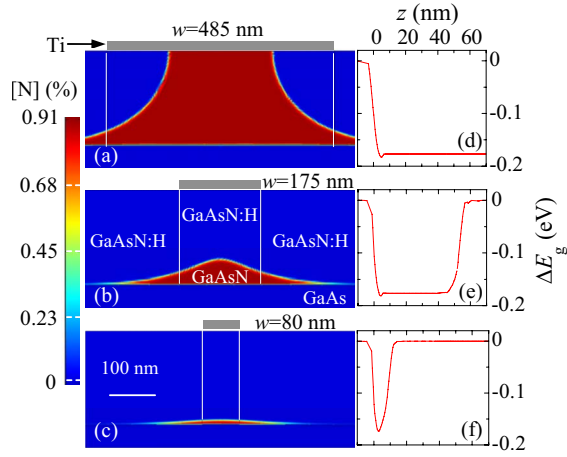


FIG. 1. (Color online) Left panels: post-hydrogenation distribution of electronically active N atoms in a sample section containing the growth axis. The wires run perpendicularly to the figure plane and the Ti wire is sketched as a gray rectangle on the top surface. Panels (a), (b), and (c) are the simulations obtained for Ti wires deposited on the  $\text{GaAs}_{1-x}\text{N}_x$  surface having width equal to  $w = 485$  nm,  $w = 175$  nm and  $w = 80$  nm, respectively. The effective N concentration is shown in a false color scale on the left. The N atom distributions are calculated by extending in two dimensions and in the presence of a Ti mask the model reported in Refs. 15 and 18. Right panels: Band gap energy modulation,  $\Delta E_g$ , along the vertical symmetry axis of the wires ( $z$  starts from the buffer/ $\text{GaAs}_{1-x}\text{N}_x$  interface,  $z = 0$  nm). (d)  $w = 485$  nm, (e)  $w = 175$  nm, (f)  $w = 80$  nm.

=600 nm) pumped by the second harmonic of a Nd:YAG pulsed laser was used for excitation; the pulse duration was 5 ps and the repetition rate 76 MHz. For light collection, a confocal microscope configuration was used with two different infinity objectives. The  $\mu$ -PL signal was then focused onto a multimode optical fiber and dispersed by a single grating spectrometer with 25 cm focal length. It was then detected by an  $\text{In}_{1-x}\text{Al}_x\text{As}/\text{In}_{1-x}\text{Ga}_x\text{As}$  photomultiplier followed by a photon counting apparatus for PL measurements and a time-correlated single-photon counting setup providing an experimental time resolution of 200 ps for time-resolved spectra.

Hydrogen diffusion profiles were simulated by solving a system of partial differential equations in two dimensions via finite-element calculations that take into account the various formation/dissolution steps involved in H kinetics in  $\text{GaAs}_{1-x}\text{N}_x$  introduced in Refs. 12, 15, and 18. In those previous works, one-dimensional deuterium diffusion profiles in bulk  $\text{GaAs}_{1-x}\text{N}_x$ , have been measured by secondary ion mass spectrometry. This allowed to develop the model and tune the relevant parameter values (*e.g.*, D diffusion coefficient and capture rate, etc.) in the case of D diffusion in presence of a very high trap density.<sup>18</sup>

### III. RESULTS AND DISCUSSION

Figures 1(a)–1(c) show the calculated distribution of unpassivated (or electronically active) N atoms in different  $\text{GaAs}_{1-x}\text{N}_x$  wires. The data refer to a section containing the

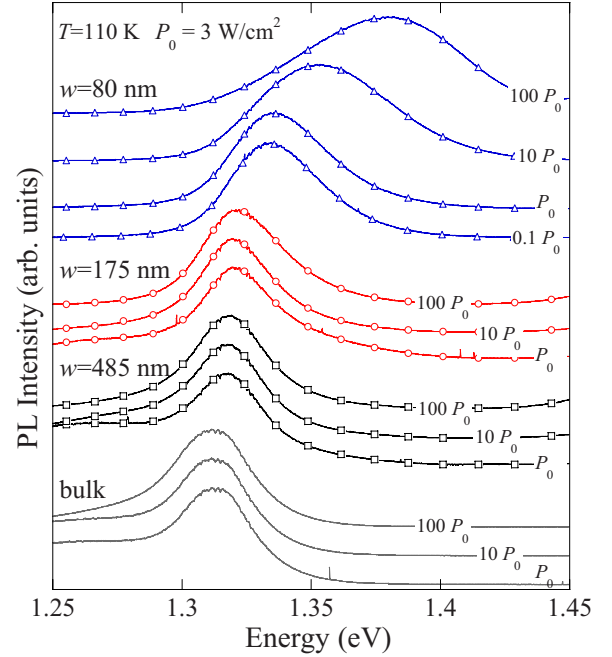


FIG. 2. (Color online) Photoluminescence spectra at  $T = 110$  K recorded for different laser power densities ( $P_0 = 3.0$  W/cm<sup>2</sup>) on bulk  $\text{GaAs}_{1-x}\text{N}_x$  (bottommost spectra) and  $\text{GaAs}_{1-x}\text{N}_x/\text{GaAs}_{1-x}\text{N}_x:\text{H}$  wires having different width,  $w$  (refer to Fig. 1).

growth axis of the sample (the section is perpendicular to the wire direction). The simulations have been obtained by extending to two dimensions the model reported in Refs. 15 and 18 (but for the presence of Ti masks that were assumed to completely block H atoms).<sup>19</sup> Initial and boundary conditions (and complex dissociation energies<sup>20</sup>) were the same used in those previous works. In the present simulations, the H-ion current impinging on the sample surface, the exposure duration to H, the irradiation temperature have been set equal to the experimental values. Hydrogen diffusion coefficient ( $D = 1.57 \times 10^{-12}$  cm<sup>2</sup>/s) and capture radius ( $r = 1$  Å) were chosen so that the H diffusion forefront coincided with the  $\text{GaAs}_{1-x}\text{N}_x/\text{GaAs}$  interface far from the wires, as verified *a-posteriori* by PL measurements. In accordance with previous (one-dimensional) studies,<sup>15,18</sup> the profile of unpassivated N atoms is estimated to be characterized by sharp interfaces, where N concentration varies from zero to its maximum value within less than 10 nm. The size and shape of the wirelike heterostructures so formed change rapidly with  $w$ . In turn, this causes a marked variation of the potential profile to which carriers are subjected. Figures 1(d)–1(f) show the spatial modulation of the band gap energy,  $\Delta E_g$ , along the growth axis  $z$  (the line scan is performed along the symmetry axis perpendicular to the wire).  $\Delta E_g$  has been determined by using the known relationship between N concentration and the  $\text{GaAs}_{1-x}\text{N}_x$  band gap energy.<sup>9,10</sup> Importantly, for  $w = 80$  nm the vertical size of the wire is about 10 nm that leads to carrier quantum confinement, as discussed in the following.

Figure 2 shows the peak-normalized PL spectra of  $\text{GaAs}_{1-x}\text{N}_x/\text{GaAs}_{1-x}\text{N}_x:\text{H}$  wire ensembles and unpatterned

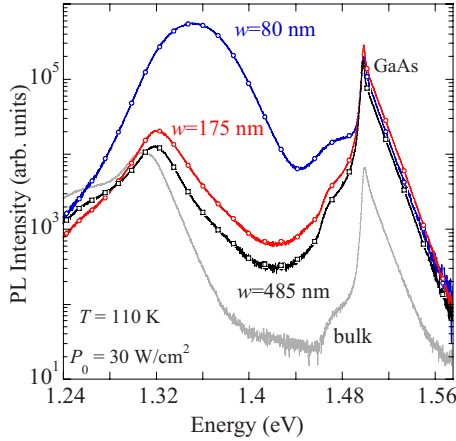


FIG. 3. (Color online) Photoluminescence spectra at  $T=110$  K recorded for a same laser power density ( $P_0=30$  W/cm $^2$ ) on bulk GaAs $_{1-x}$ N $_x$  (bottommost spectra) and GaAs $_{1-x}$ N $_x$ /GaAs $_{1-x}$ N $_x$ :H wires having different width,  $w$  (refer to Fig. 1). Notice the large increase in the PL signal from GaAs $_{1-x}$ N $_x$  in the narrowest wire.

GaAs $_{1-x}$ N $_x$  for different laser powers  $P$ . The lattice temperature was 110 K in order to highlight the free-exciton recombination with respect to that from localized states,<sup>21</sup> whose contribution appears as a weak low-energy component rapidly decreasing for increasing  $P$ . No other major variation in the PL lineshape is noticed with increasing  $P$  in the unpatterned sample and in the two widest wires.

A blueshift of the PL peak energy with respect to the bulk sample is observed for all wire sizes. The small value ( $\sim 5$ – $8$  meV) it has in the  $w=485$  and  $175$  nm wires is due to strain fields generated by the lattice expansion of the GaAs $_{1-x}$ N $_x$ :H barriers, as discussed in Ref. 17. However, in the  $w=80$  nm wire such a blueshift amounts to  $\sim 25$  meV for  $0.1P_0 \leq P \leq P_0$  and still to  $\sim 20$  meV after subtracting strain contribution.<sup>22</sup> The latter value well matches the quantum confinement energy as estimated for a 10 nm-thick GaAs $_{1-x}$ N $_x$  ( $x=0.9\%$ ) quantum well sandwiched in GaAs barriers [10 nm is the average thickness of the GaAs $_{1-x}$ N $_x$  wire as it results from the data displayed in Fig. 1(f)]. This provides a first evidence of carrier confinement in the narrowest wires. Eventually, the blueshift raises to  $\sim 65$  meV for  $P=100 P_0$  (see topmost spectra in Fig. 2) as a consequence of the reduced recombining volume and hence of the increased photoexcited carrier density in the smallest wires.

Figure 3 shows the PL spectra of different wires recorded under the same laser excitation intensity (the spectrum of the GaAs $_{1-x}$ N $_x$  bulk is shown, too). On going from the bulk to the  $w=485$  nm PL spectrum, the GaAs $_{1-x}$ N $_x$  signal is roughly constant while the GaAs integrated PL intensity increases by a factor  $\sim 30$ , due to the conversion of the hydrogenated GaAs $_{1-x}$ N $_x$  into a GaAs-like material. In the case of the 175 nm structures, the integrated intensities of the “GaAs” and GaAs $_{1-x}$ N $_x$  signal raise slightly with respect to  $w=485$  nm by an amount equal to  $\sim 1.1$  and  $\sim 1.6$ , respectively. In the case of the 80 nm wires, instead, the GaAs $_{1-x}$ N $_x$  integrated intensity increases dramatically by a factor of  $\sim 35$  ( $\sim 60$ ) and blueshifts compared to  $w=175$  nm (bulk) despite the overall decreased GaAs $_{1-x}$ N $_x$  volume. At the same time, the “GaAs” signal remains about equal to that found in the

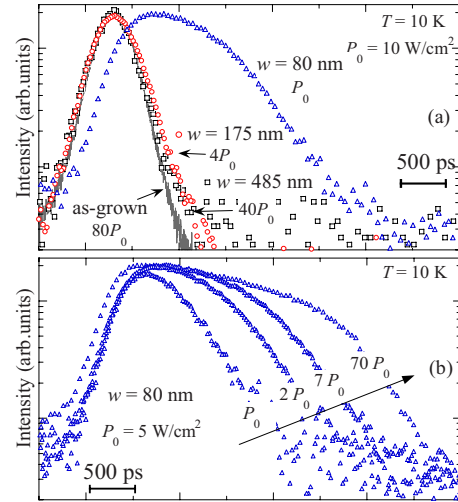


FIG. 4. (Color online) (a) Low-temperature ( $T=10$  K) time-resolved microphotoluminescence ( $\mu$ -PL) spectra on single wires having width  $w$  equal to 485, 175, 80 nm (squares, circles and triangles, respectively) and on the unpatterned sample (solid line), as obtained by setting the detection energy at the free-exciton recombination energy. Different laser power densities have been used in order to obtain the same density of collected photogenerated carriers in the different wires (as explained in the text). (b) Time resolved  $\mu$ -PL spectra on a single 80 nm wire as a function of the excitation power.

larger wires. This increase in the GaAs $_{1-x}$ N $_x$  PL integrated intensity for constant number of photoexcited carriers has to be attributed to an enhanced radiative efficiency, a signature of an increased electron-hole wave function overlap due to sizable carrier confinement in the nanostructures.

We now address these confinement effects by studying carrier dynamics in single heterostructures. Figure 4 shows the time evolution of the emission at  $T=10$  K of different single wires (symbols) and of the unpatterned sample (solid line). The detection energy is set at the maximum of the free-exciton band, as measured by continuous-wave  $\mu$ -PL (consequently localized states are not involved in the data of Fig. 4). Different laser power densities were used for different  $w$ 's in order to obtain a same density of photogenerated carriers and thus to compare carrier dynamics consistently in the various structures. In fact, according to the simulations shown in Figs. 1(a)–1(c), it is found that the space region where carriers recombine reduces by a factor about 10 and 40 on going from  $w=485$  nm to  $w=175$  and 80 nm, respectively (no major role is played by the carrier diffusion length,  $\sim 1$   $\mu$ m,<sup>14</sup> which is sizably larger than the widest wire considered). The behavior of the  $w=485$  and 175 nm wires is similar to that of the as-grown sample: The three decay curves overlap in Fig. 4. Instead, for  $w=80$  nm the  $\mu$ -PL intensity exhibits an overall longer decay. A plateau clearly develops by increasing the excitation power [see Fig. 4(b)] or by moving the detection energy on the low-energy side of the PL free-exciton band (not shown here), as also reported for quantum dots.<sup>23,24</sup> These behaviors are absent in the 485

nm wires and are much less evident in the 175 nm wires. In the lowest excitation regime achieved, the time evolution of the emission from the 80 nm wires is eventually monoexponential, with a decay time being slightly longer with respect to the thicker wires and the as-grown sample. The plateau displayed in the  $w=80$  nm wire is a fingerprint of band-filling effects, which usually take place in low-dimensional systems because of a reduced density of states.<sup>23,24</sup> In fact, carrier replenishment of the ground state from higher-energy states is slowed down by the breaking-up of the bulk continuum levels into discrete levels (along one dimension at least in our case), that is a consequence of quantum confinement.

#### IV. CONCLUSIONS

In summary, we investigated the electronic properties of H-structured  $\text{GaAs}_{1-x}\text{N}_x/\text{GaAs}$  wires having different width. In the case of the narrowest wires, continuous-wave PL spectra show an increase in the energy of the ground state and in the PL efficiency. In the same wires, time-resolved  $\mu\text{-PL}$  displays a strong slow down of the whole carrier recombination dynamics. The experimental scenario can be accounted for by the occurrence of carrier quantum confinement. Therefore, these results show that a H-mediated nanostructuring of dilute nitrides is feasible in two dimensions thus featuring promising prospects for the attainment of zero-dimensional carrier confinement in a fully controllable engineered way.

\*antonio.polimeni@roma1.infn.it

- <sup>1</sup>S. Kiravittaya, A. Rastelli, and O. G. Schmidt, *Rep. Prog. Phys.* **72**, 046502 (2009).
- <sup>2</sup>J. Stangl, V. Holý, and G. Bauer, *Rev. Mod. Phys.* **76**, 725 (2004).
- <sup>3</sup>Q. Zhu, K. F. Karlsson, E. Pelucchi, and E. Kapon, *Nano Lett.* **7**, 2227 (2007).
- <sup>4</sup>M. S. Gudixsen, L. J. Lauhon, J. Wang, D. C. Smith, and C. M. Lieber, *Nature (London)* **415**, 617 (2002).
- <sup>5</sup>*Dilute Nitride Semiconductors*, edited by M. Henini (Elsevier, Oxford, UK, 2005).
- <sup>6</sup>A. Polimeni, G. Baldassarri H. v., H. M. Bissiri, M. Capizzi, M. Fischer, M. Reinhardt, and A. Forchel, *Phys. Rev. B* **63**, 201304(R) (2001).
- <sup>7</sup>A. Polimeni, M. Bissiri, M. Felici, M. Capizzi, I. A. Buyanova, W. M. Chen, H. P. Xin, and C. W. Tu, *Phys. Rev. B* **67**, 201303(R) (2003).
- <sup>8</sup>A. Polimeni, G. Baldassarri Hoeger von Hoegersthal, F. Masia, A. Frova, M. Capizzi, S. Sanna, V. Fiorentini, P. J. Klar, and W. Stolz, *Phys. Rev. B* **69**, 041201(R) (2004).
- <sup>9</sup>F. Masia, G. Pettinari, A. Polimeni, M. Felici, A. Miriametro, M. Capizzi, A. Lindsay, S. B. Healy, E. P. O'Reilly, A. Cristofoli, G. Bais, M. Piccin, S. Rubini, F. Martelli, A. Franciosi, P. J. Klar, K. Volz, and W. Stolz, *Phys. Rev. B* **73**, 073201 (2006).
- <sup>10</sup>G. Pettinari, F. Masia, A. Polimeni, M. Felici, A. Frova, M. Capizzi, A. Lindsay, E. P. O'Reilly, P. J. Klar, W. Stolz, G. Bais, M. Piccin, S. Rubini, F. Martelli, and A. Franciosi, *Phys. Rev. B* **74**, 245202 (2006).
- <sup>11</sup>P. J. Klar, H. Grüning, M. Güngerich, W. Heimbrodt, J. Koch, T. Torunski, W. Stolz, A. Polimeni, and M. Capizzi, *Phys. Rev. B* **67**, 121206(R) (2003).
- <sup>12</sup>M. Berti, G. Bisognin, D. DeSalvador, E. Napolitani, S. Vangelista, A. Polimeni, M. Capizzi, F. Boscherini, G. Ciatto, S. Rubini, F. Martelli, and A. Franciosi, *Phys. Rev. B* **76**, 205323 (2007).
- <sup>13</sup>F. Jiang, M. Stavola, M. Capizzi, A. Polimeni, A. Amore Bonapasta, and F. Filippone, *Phys. Rev. B* **69**, 041309(R) (2004).
- <sup>14</sup>M. Felici, A. Polimeni, G. Salviati, L. Lazzarini, N. Armani, F. Masia, M. Capizzi, F. Martelli, M. Lazzarino, G. Bais, M. Piccin, S. Rubini, and A. Franciosi, *Adv. Mater.* **18**, 1993 (2006).
- <sup>15</sup>R. Trotta, A. Polimeni, M. Capizzi, D. Giubertoni, M. Bersani, G. Bisognin, M. Berti, S. Rubini, F. Martelli, L. Mariucci, M. Francardi, and A. Gerardino, *Appl. Phys. Lett.* **92**, 221901 (2008).
- <sup>16</sup>L. Felisari, V. Grillo, F. Martelli, R. Trotta, A. Polimeni, M. Capizzi, F. Jabeen, and L. Mariucci, *Appl. Phys. Lett.* **93**, 102116 (2008).
- <sup>17</sup>R. Trotta, A. Polimeni, M. Capizzi, F. Martelli, S. Rubini, M. Francardi, A. Gerardino, and L. Mariucci, *Appl. Phys. Lett.* **94**, 261905 (2009).
- <sup>18</sup>R. Trotta, D. Giubertoni, A. Polimeni, M. Bersani, M. Capizzi, F. Martelli, S. Rubini, G. Bisognin, and M. Berti, *Phys. Rev. B* **80**, 195206 (2009).
- <sup>19</sup>It may be worth noticing that these calculations qualitatively reproduce also the results obtained in GaAs in two dimension by D. P. Kennedy and R. R. O'Brien, *IBM J. Res. Dev.* **9**, 179 (1965).
- <sup>20</sup>G. Bisognin, D. De Salvador, E. Napolitani, M. Berti, A. Polimeni, M. Capizzi, S. Rubini, F. Martelli, and A. Franciosi, *J. Appl. Crystallogr.* **41**, 366 (2008).
- <sup>21</sup>A. Polimeni, M. Capizzi, M. Geddo, M. Fischer, M. Reinhardt, and A. Forchel, *Appl. Phys. Lett.* **77**, 2870 (2000).
- <sup>22</sup>As reported in Ref. 17, the extent of the energy shift induced by strain saturates for  $w < 500$  nm. Thus, in the  $w=80$  nm wire it can be safely assumed equal to 5 meV.
- <sup>23</sup>V. Zwiller, M.-E. Pistol, D. Hessman, R. Cederström, W. Seifert, and L. Samuelson, *Phys. Rev. B* **59**, 5021 (1999).
- <sup>24</sup>P. Castrillo, D. Hessman, M.-E. Pistol, N. Carlsson, and L. Samuelson, *Appl. Phys. Lett.* **67**, 1905 (1995).